Performance of MISO Time Reversal Ultra-wideband over an 802.15.3a Channel Model

Bruno A. Angélico,
Phillip M. S. Burt,
Paul Jean E. Jeszensky
Dept. of Telecommunications
and Control Engineering
Escola Politécnica of the University of São Paulo
Brazil. e-mail: angelico@lcs.poli.usp.br;
phillip@lcs.poli.usp.br; pjj@lcs.poli.usp.br

William S. Hodgkiss
Dept. of Electrical &
Computer Engineering
University of California San Diego
e-mail: whodgkiss@ucsd.edu

Taufik Abrão
Dept. of Electrical Engineering
State University of Londrina
Brazil. e-mail: taufik@uel.br

***Abstract*—This paper analyzes the performance of a baseband multiple-input single-output (MISO) time reversal ultra-wideband system (TR-UWB) over the IEEE 802.15.3a channel model. Two scenarios are considered, CM1 based on LOS (0-4m) channel measurements and CM3 based on NLOS (4-10m) channel measurements. A semi-analytical performance expression is derived and compared with simulation results in terms of the number of antenna elements, number of users, and transmission rate. The results show that the system performance is improved with an increase in the number of transmit antenna elements and that additional equalization and multiple access enhancement schemes are necessary for high transmission rates.**

I. Introduction

UWB recently has been considered with great interest due to some attractive characteristics, such as very high data rates, low probability of interception, and good time domain resolution allowing location and tracking applications at centimeter level. Potential applications of UWB include wireless personal area networks, wireless sensor networks, imaging systems, and vehicular radar systems [1].

In February 2002, the Federal Communications Commission (FCC) announced the FCC First Report and Order (R&O) [2] that permitted the deployment of UWB devices for data communications over an enormous bandwidth from 3.1 to 10.6 GHz. The FCC rules do not define a specific technology. Three UWB categories were specified: imaging systems, communications and measurements, and vehicular radar systems.

There is a growing interest in applying time reversal to wireless communications [3], resulting in the following advantages: inter-symbol interference (ISI) mitigation by reducing the delay spread of the channel (temporal focusing), and co-channel interference (or multiple access interference — MAI) rejection by focusing the signal on the point of interest (spatial focusing). This can be done estimating the channel impulse response (CIR) from a probe signal, and convolving the data to be transmitted with the complex conjugate time reversed version of the estimated CIR. TR-UWB exploits the UWB channel reciprocity, which was experimentally verified in [4] for a particular UWB scenario. The authors in [4] also found that, for a MISO UWB system under a particular scenario, the spacing of 20 cm is sufficient for ensuring no correlation between antenna elements.

This work considers a baseband model of a time reversal system with multiple transmit antennas and a single or multiple users with a single antenna accessing the system simultaneously. It is assumed that the transmission is from a base station with relatively good computational capacity to a lower complexity device with hardware constraints, similar to a downlink communication system. Independent channel realizations per antenna, perfect channel estimation, and perfect synchronization at the receiver are ideally assumed. The paper is organized as follows: the system model is described in Section II and the signal-to-interference-plus-noise ratio ($SINR$) analysis is presented in Section III. Section IV describes the channel model and the time reversal temporal coefficients. The performance results are shown in Section V, and the main conclusions are pointed out in Section VI.

II. System Model

The adopted baseband transmitted pulse shape has a square-root raised cosine form given by [5]

$$g_T(t)=\begin{cases}\frac{1}{\sqrt{T}}\frac{\sin[\pi(1-\alpha)t/T]+(4\alpha t/T)\cos[\pi(1+\alpha)t/T]}{(\pi t/T)\left[1-(4\alpha t/T)^2\right]}, & t\neq 0, t\neq \frac{T}{4\alpha}\\ \frac{1}{\sqrt{T}}\left[1-\alpha+\frac{4\alpha}{\pi}\right], & t=0\\ \frac{\alpha}{\sqrt{2T}}\left[\left(1+\frac{2}{\pi}\right)\sin\left(\frac{\pi}{4\alpha}\right)+\left(1-\frac{2}{\pi}\right)\cos\left(\frac{\pi}{4\alpha}\right)\right], & t=\pm\frac{T}{4\alpha}\end{cases}, \tag{1}$$

where T is the reciprocal of the symbol rate, and α is the roll-off factor. In this work the parameter T is kept constant for the pulse shape generation, but the effective symbol rate is controlled by the space between consecutive symbols given by $T_s = \kappa T$, where κ is an integer. Considering an antipodal binary signaling with symbols $b_u^i \in \{\pm 1\}$, the uth user's signal before time reversal convolution is given by

$$s_u(t) = \sum_{i=-\infty}^{\infty} b_u^i \, g_T(t - iT_s) \tag{2}$$

As in [6], a MISO multiuser time reversal system is considered (Figure 1). Basically, there are three steps in this TR communication. First, a pilot signal is transmitted

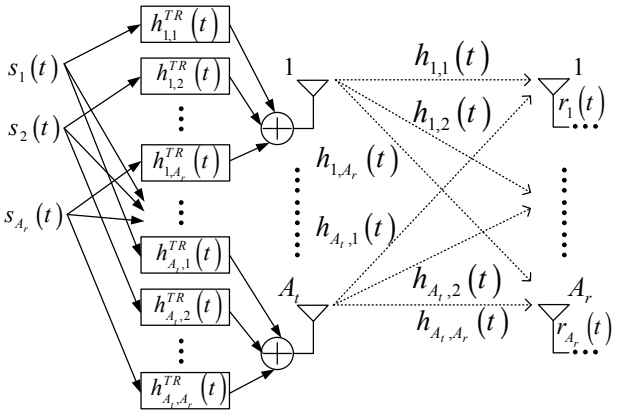

Fig. 1. Multi-user (or MIMO) TR communication system with A_t transmit antennas and A_r users (or receive antennas).

from the uth receive to the kth transmit element in order to sound the propagation channel with its channel impulse response, $h_{k,u}(t)$. Second, the transmitter records the received signal and estimates the channel coefficients. Third, the signal to be transmitted, $s_u(t)$, is convolved with the TR signal $h_{k,u}^{TR}(t) = h_{k,u}^{*}(-t)$. If the channel is perfectly reciprocal and slowly varying, the equivalent baseband uth received signal can be represented by

$$r_u(t) = s_u(t) * \sum_{k=1}^{A_t} h_{k,u}^{TR}(t) * h_{k,u}(t) + \sum_{k=1}^{A_t} \sum_{\substack{q=1 \\ q \neq u}}^{A_r} s_q(t) * h_{k,q}^{TR}(t) * h_{k,u}(t) + \eta(t), \quad (3)$$

where A_t and A_r are the number of transmit and receive antennas (A_r users), $s_u(t)$ and $s_q(t)$ are the transmitted signal intended for the uth user (or receive antenna) and for the qth user (or receive antenna). The symbol $*$ denotes the convolution operator, while $\eta(t)$ represents the equivalent complex baseband Additive White Gaussian Noise (AWGN). Note that if the channel is perfectly estimated at the transmitter side, $h_{k,u}^{TR}(t) * h_{k,u}(t) = R_{k,u}^{auto}$ is the autocorrelation of $h_{k,u}(t)$, and $h_{k,q}^{TR}(t) * h_{k,u}(t) = R_{k,q,u}^{cross}$ is the cross correlation between $h_{k,q}(t)$ and $h_{k,u}(t)$.

In [7] the authors showed that multiple transmit antennas increase the ratio between the peak and the side lobes of the equivalent CIR in a time reversal system[1], reducing ISI. This is due to the fact that, in the sum of autocorrelations, the peaks add up coherently and the side lobes add incoherently at the receive element.

If different taps of the channel impulse response are statistically independent, the autocorrelation will be more focused in time and more energy of the signal will be concentrated at the peak of the autocorrelation, reducing the ISI. Also, if each communication link is independent and unique, the desired signal at the receive element will be enhanced and the cross-channel interference attenuated, resulting in spatial focusing. However, for high data transmission rates, even if the CIR is perfectly known at the receiver, the ISI will degrade the system performance, because the $R_{k,u}^{auto}$ is not a delta function. In addition, if the channel multipaths are somewhat correlated or there is a slight change in the environment over the propagation path, additional ISI will be introduced. To handle such impairments, a channel equalization scheme can be employed with fewer taps than that used without TR [8].

[1]In this case, the term equivalent CIR refers to: $\sum_{k=1}^{A_t} h_{k,u}^{TR}(t) * h_{k,u}(t)$.

III. Signal-to-Interference-Plus-Noise Ratio Analysis and BER Performance

A. $SINR$ Derivation

At the receiver side, the received signal is subjected to a filter $g_R(t)$ matched to the pulse $g_T(t)$. Hence, the transmitted signal passes through two matched filters (MF): one matched to the CIR and another matched to the pulse shape at the receiver. The output of the receiver filter for the uth user is

$$\begin{aligned} y_u(t) &= s_u(t) * \sum_{k=1}^{A_t} h_{k,u}^{TR}(t) * h_{k,u}(t) * g_R(t) + \\ &+ \sum_{\substack{q=1 \\ q \neq u}}^{A_r} s_q(t) * \sum_{k=1}^{A_t} h_{k,q}^{TR}(t) * h_{k,u}(t) * g_R(t) + \underbrace{\eta(t) * g_R(t)}_{z(t)} = \\ &= \sum_{i=-\infty}^{\infty} b_u^i \underbrace{g_T(t - iT_s) * \sum_{k=1}^{A_t} h_{k,u}^{TR}(t) * h_{k,u}(t) * g_R(t)}_{x_u(t-iT_s)} + \\ &+ \sum_{i=-\infty}^{\infty} \sum_{\substack{q=1 \\ q \neq u}}^{A_r} b_q^i \underbrace{g_T(t - iT_s) * \sum_{k=1}^{A_t} h_{k,q}^{TR}(t) * h_{k,u}(t) * g_R(t)}_{f_{u,q}(t-iT_s)} + \\ &+ z(t) = \\ &= \sum_{i=-\infty}^{\infty} b_u^i x_u(t - iT_s) + \sum_{i=-\infty}^{\infty} \sum_{\substack{q=1 \\ q \neq u}}^{A_r} b_q^i f_{u,q}(t - iT_s) + z(t) \end{aligned} \quad (4)$$

If the matched filter output at the receiver is sampled with rate $1/T_s$, it becomes

$$y_u(nT_s) = \sum_{i=-\infty}^{\infty} b_u^i x_u([n-i]T_s) + \sum_{i=-\infty}^{\infty} \sum_{\substack{q=1 \\ q \neq u}}^{A_r} b_q^i f_{u,q}([n-i]T_s) + z(nT_s) \quad (5)$$

With the change of variable, $v = n - i \Rightarrow i = n - v$, it follows that

$$y_u(nT_s) = \sum_{v=\infty}^{-\infty} b_u^{n-v} x_u(vT_s) + \sum_{v=\infty}^{-\infty} \sum_{\substack{q=1 \\ q \neq u}}^{A_r} b_q^{n-v} f_{u,q}(vT_s) + z(nT_s), \quad (6)$$

which can be rewritten as

$$y_u(nT_s) = \underbrace{b_u^n x_u(0)}_{\text{Signal}} + \underbrace{\sum_{\substack{v=-\infty \\ v\neq 0}}^{\infty} b_u^{n-v} x_u(vT_s)}_{\text{ISI}} + \underbrace{\sum_{\substack{q=1 \\ q\neq u}}^{A_r} \sum_{v=-\infty}^{\infty} b_q^{n-v} f_{u,q}(vT_s)}_{\text{MAI}} + \underbrace{z(nT_s)}_{\text{Noise}} \quad (7)$$

In this notation, $v = 0$ represents the timing of the peak of $x_u(v)$, which is assumed to be perfectly synchronized at the receiver. For this complex baseband representation with complex transmission and binary antipodal signaling, if the CIR is perfectly estimated, the desired signal in (7) is real, while the residual ISI and MAI are still complex. Note that the discrete-time sequence that represents the sampled noise $z(nT_s) = z_n$ is still AWGN, and its variance (or power) is defined as σ_d^2. Hence, the variance of the in-phase and quadrature components of z_n are equal and given by $\sigma^2 = \sigma_d^2/2$ [9]. The decision variable is given by

$$V_u = \Re\{y_u(nT_s)\} \quad (8)$$

The signal-to-interference-plus-noise ratio of the uth user conditioned on the jth set of channel realizations is given by Equation (9) (at the top of next page), where $\mathbb{E}[\cdot]$ denotes the expected value operator. If the information symbols are independent and identically distributed (i.i.d.), Equation (9) can be rewritten as Equation (10). Without loss of generality σ_b^2 can be fixed as $\sigma_b^2 = 1$, and Equation (10) results in

$$SINR_u^j = \frac{\Re\{x_u^j(0)\}^2}{\sum_{\substack{v=-\infty \\ v\neq 0}}^{\infty} \Re\{x_u^j(vT_s)\}^2 + \sum_{\substack{q=1 \\ q\neq u}}^{A_r} \sum_{v=-\infty}^{\infty} \Re\{f_{u,q}^j(vT_s)\}^2 + \sigma^2} \quad (11)$$

From Equation (11) it is possible to see that the higher the transmission rate, the higher the ISI and MAI, and the lower the $SINR$.

B. Noise Calibration, MF Bound and BER Performance

Defining the signal-to-noise ratio (SNR) at the output of the matched filter as

$$SNR = \frac{Eb_d}{\sigma_d^2} = \frac{Eb_d}{2\,\sigma^2}, \quad (12)$$

where $Eb_d = |x_u(0)|^2$ is here defined as the bit energy (peak energy) after MF, the variance of the in-phase and quadrature components of z_n are obtained as

$$\sigma^2 = \frac{Eb_d}{2\,SNR} \quad (13)$$

The single-user matched filter bound for antipodal binary signaling is then given by

$$SuB = Q\left(\sqrt{2\,SNR}\right) = Q\left(\sqrt{\frac{2Eb_d}{\sigma_d^2}}\right), \quad (14)$$

where $Q(x) = \frac{1}{\sqrt{2\pi}} \cdot \int_x^{\infty} e^{-y^2/2}\,dy$. If the ISI and the MAI after MF in Equation (11) can be considered Gaussian distributed, the bit error ratio (BER) for the uth user conditioned to the jth set of channel realizations is

$$BER_u^j = Q\left(\sqrt{SINR_u^j}\right) \quad (15)$$

Considering J sets of channel realizations and A_r equal power users, the average BER can be computed as

$$BER = \frac{1}{J \cdot A_r} \sum_{u=1}^{A_r} \sum_{j=1}^{J} BER_u^j \quad (16)$$

Note that the definition of SNR discussed above, which is based on [6], does not emphasize the array gain of the MISO system, because the noise power is calculated according to the peak energy (or power) of the equivalent CIR at the receiver, but not according to the energy (or power) per antenna.

IV. Channel Model and Time Reversal Filter

A. Channel Model

The channel modeling subcommittee of the TG3a recommended a channel model that is basically a modified version of the Saleh-Valenzuela (mSV) model [10], [11], [12], where multipath components (MPCs) arrive at the receiver in clusters. Cluster arrivals are Poisson distributed with rate Λ. The ray arrivals within each cluster are also a Poisson process with rate $\lambda > \Lambda$. The arrival time of the mth cluster is denoted by τ_m, and the arrival time of the nth ray within the mth cluster by $\tau_{m,n}$. The channel coefficient (path) gain $\beta_{m,n}$ is a real-valued random variable with magnitude described by a log-normal distribution and its phase is constrained to take only values 0 or π with equal probability. Four scenarios were proposed in [10]: CM1 – based on line of sight (LOS) 0-4m channel measurements, CM2 – based on non-LOS (NLOS) 0-4m measurements, CM3 – based on NLOS 4-10m measurements, and CM4 based on an extreme NLOS environment. The present work considers the CM1 and CM3 scenarios. One multipath channel realization consists of cluster arriving rays:

$$h_c(t) = \chi \sum_{m=0}^{M} \sum_{n=0}^{N} \beta_{m,n}\,\delta(t - \tau_m - \tau_{m,n}) \quad (17)$$

where δ is the Dirac delta function and χ represents the log-normal shadowing term. The above described CIR is not a baseband complex tap model and its output is a continuous time arrival and amplitude value.

B. Discrete-time Baseband Channel and TR Coefficients

The channel characteristics provided in [10], [11] are based on a $ts = 167$ ps sampling time. An arbitrary realization of the channel with multipath resolution ts can be represented as the following periodic impulse train

$$h'(t) = \chi \sum_{\ell=0}^{L} \beta_\ell\,\delta(t - \tau_\ell), \quad (18)$$

$$SINR_u^j = \frac{\mathbb{E}\left[\Re\left\{b_u^n x_u^j(0)\right\}^2\right]}{\mathbb{E}\left[\Re\left\{\sum\limits_{\substack{v=-\infty\\v\neq 0}}^{\infty} b_u^{n-v} x_u^j(vT_s)\right\}^2\right] + \mathbb{E}\left[\Re\left\{\sum\limits_{\substack{q=1\\q\neq u}}^{A_r}\sum\limits_{v=-\infty}^{\infty} b_q^{n-v} f_{u,q}^j(vT_s)\right\}^2\right] + \sigma^2} \tag{9}$$

$$SINR_u^j = \frac{\sigma_b^2 \Re\left\{x_u^j(0)\right\}^2}{\sigma_b^2 \sum\limits_{\substack{v=-\infty\\v\neq 0}}^{\infty} \Re\left\{x_u^j(vT_s)\right\}^2 + \sigma_b^2 \sum\limits_{\substack{q=1\\q\neq u}}^{A_r}\sum\limits_{v=-\infty}^{\infty} \Re\left\{f_{u,q}^j(vT_s)\right\}^2 + \sigma^2} \tag{10}$$

where $\tau_\ell = \ell\, ts$. In this paper, a baseband signal analysis is adopted. Thus, since the mSV is a bandpass channel model, its complex baseband version must be generated. The discrete-time baseband CIR with sampling time T is obtained by

$$\begin{aligned} h_d[nT] &= \int_{-\infty}^{\infty} p(nT-t)\, h'(t)\, e^{-j\omega_c t}\, \mathrm{d}t \\ &= \chi \sum_{\ell=0}^{L} p(nT-\tau_\ell)\, \beta_\ell e^{-j\omega_c \tau_\ell}, \end{aligned} \tag{19}$$

where $p(t) = g_T(t) * g_R(t)$, and $g_T(t)$ is the pulse shape defined by Equation (1) with roll-off factor $\alpha = 0.3$ and $T = 3\,ts = 501$ ps. The down-conversion process is performed by the term $\mathrm{e}^{-j2\pi f_c t}$ with the carrier center frequency $f_c = 4.1$ GHz. Additionally, the channel coefficients are normalized to unity energy, which means that the shadowing factor is not taken into account. The resultant discrete-time complex baseband CIR is used in order to obtain the simulation results and also to derive the semi-analytical performances. Note that the pulse shape filter is already included in the discrete-time baseband CIR [13].

The TR filter considers that the CIR is perfectly estimated at the transmitter. Figure 2 illustrates the compression of the CIR after time reversal for an arbitrary realization of the scenarios CM1 and CM3.

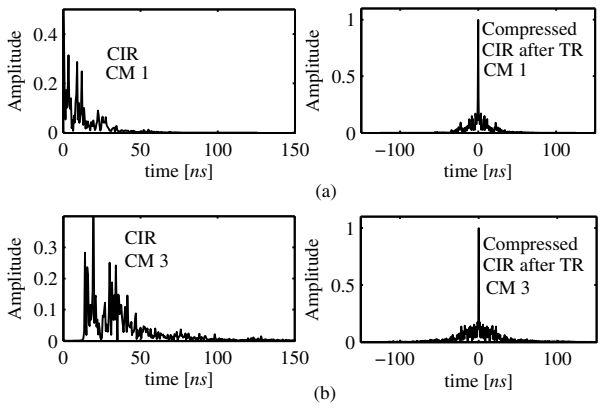

Fig. 2. Magnitude of complex resampled baseband CIR and compressed CIR after time reversal for (a) CM1, and (b) CM3.

V. Simulation Configuration and Results

A baseband Monte Carlo simulation (MCS) method is adopted with four different transmission rates $Rb = 1/Ts$, where $T_s = \kappa T$: 31.19 Mbps ($\kappa = 64$ — Rate A), 124.75 Mbps ($\kappa = 16$ — Rate B), 499 Mbps ($\kappa = 4$ — Rate C), and 998 Mbps ($\kappa = 2$ — Rate D), where $T = 3\,ts = 501$ ps. The signal at the output of the receiver matched filter is sampled at a rate equal to $1/T_s$. The transmitted frame has a duration of $T_f = 100$ μs. During a frame interval the channel remains static. As the pulse shape filter is already included in the coefficients $h_d[nT]$, the signal to be transmitted is generated by simply convolving the information symbols[2] with the TR coefficients, and the receiver MF is implemented by sampling the received sequence with a sampling time given by T_s. The simulation model for a single user case (user #1, no MAI) is shown in Figure 3. $h_{d\,k,1}$ represents the CIR on the kth antenna of the user #1.

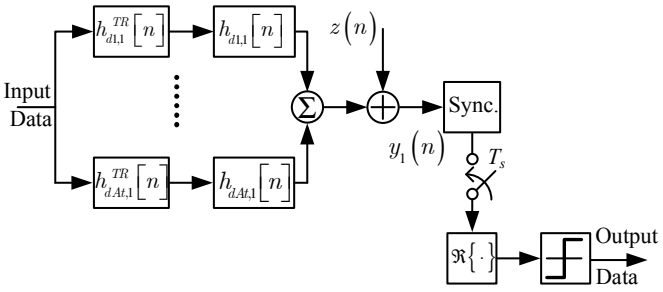

Fig. 3. Equivalent simulation model considering a single user (user #1).

Three different user loadings are considered: 1 user, 3 users, and 5 users. The channel impulse responses are randomly chosen among 100 realizations proposed in [10]. At least 200 different sets of random choices are considered for the average BER calculation in each SNR simulated point. BER performance results are shown in Figures 4, 5, and 6. In the configuration Rate A, the single user's performance is close to the AWGN SuB. For a single user, the performance in the CM1 is equal or somewhat better than in CM3. With an increase in the number of users, the performance in CM3 overcomes the performance in CM1, mainly in the configurations Rate A and Rate B, due to the fact that the CM3 has a better MAI rejection than CM1 for perfect CIR estimation (free of noise). In both channels, the system performance gets better with an increase in the number of antenna elements. In the two highest transmission rates (Rate C and Rate D), the performance over CM1 and CM3 are equivalent and degraded, especially for 3 and 5 users.

The semi-analytical performance results (THEO) from Equation (16) are also considered in Figures 4 to 6, with

[2]There are $(\kappa - 1)$ zero samples between each information symbol.

$J = 3000$ sets of channel realizations. Note that, in most of the cases, these results are close to the Monte Carlo simulation results. However, such approximation is not very accurate in some cases for 3 users in the configurations Rate A and Rate B, and for 5 users in the configurations Rate A, especially for SNR $\geq$ 9 dB.

VI. Conclusions

This paper presented a performance analysis for a MISO TR-UWB system. Due to the ideal conditions assumed for this analysis, the results obtained here may be interpreted as lower bound performances. From the results, one can see that the TR-UWB system has a good MAI and ISI rejection for relatively low rates, and that the performance gets better when the number of antennas increases. In most of the cases considered, the Gaussian assumption for the MAI and ISI terms represents a good approximation for the BER analysis. For high data rates, some schemes such as equalization and multiple access enhancement must be used in order to properly combat ISI and MAI.

References

[1] L. Yang and G. B. Giannakis, "Ultra-wideband communications: an idea whose time has come," *IEEE Signal Processing Magazine*, vol. 21, no. 6, pp. 26 – 54, Nov. 2004.

[2] FCC, "FCC First Report and Order: In the matter of Revision of Part 15 of the Commission's Rules Regarding Ultra-Wideband Transmission Systems," *FCC 02-48*, April 2002.

[3] H. T. Nguyen, J. B. Andersen, and G. F. Pedersen, "The potential use of time reversal techniques in multiple element antenna systems," *IEEE Communications Letters*, vol. 9, no. 1, pp. 40 – 42, Jan. 2005.

[4] R. C. Qiu, C. Zhou, N. Guo, and J. Q. Zhang, "Time reversal with miso for ultrawideband communications: Experimental results," *IEEE Antennas and Wireless Propagation Letters*, vol. 5, no. 1, pp. 269 – 273, Dec. 2006.

[5] J. B. Anderson, *Digital Transmission Engineering*, 2^{nd} ed. IEEE Series on Digital & Mobile Comm. - John Wiley & Sons, 2005.

[6] H. T. Nguyen, I. Z. Kovács, and P. C. F. Eggers, "A time reversal transmission approach for multiuser uwb communications," *IEEE Transactions on Antennas and Propagation*, vol. 54, no. 11, pp. 3216 – 3224, Nov. 2006.

[7] H. T. Nguyen, J. B. Andersen, G. F. Pedersen, P. Kyritsi, and P. C. F. Eggers, "Time reversal in wireless communications: a measurement-based investigation." *IEEE Transactions on Wireless Communications*, vol. 5, no. 8, pp. 2242–2252, Aug. 2006.

[8] H. C. Song, W. S. Hodgkiss, W. A. Kuperman, M. Stevenson, and T. Akal, "Improvement of time-reversal communications using adaptive channel equalizers," *IEEE Journal of Oceanic Engineering*, vol. 31, no. 2, pp. 487 – 496, Apr. 2006.

[9] W. Zhang and M. J. Miller, "Baseband equivalents in digital communication system simulation," *IEEE Transactions on Education*, vol. 35, no. 4, pp. 376–382, Nov. 1992.

[10] J. R. Foerster, "Channel Modeling Sub-committee Report Final," IEEE P802.15-02/368r5-SG3a, IEEE P802.15 Working Group for Wireless Personal Area Networks (WPAN), Dec. 2002.

[11] A. F. Molisch, J. R. Foerster, and M. Pendergrass, "Channel models for ultrawideband personal area networks," *IEEE Wireless Communications*, vol. 10, no. 6, pp. 14 – 21, Dec. 2003.

[12] A. Saleh and R. A. Valenzuela, "A statistical model for indoor multipath propagation," *IEEE J. Selected Areas Comm.*, vol. 5, no. 2, pp. 128–137, Feb. 1987.

[13] E. Torabi, J. Mietzner, and R. Schober, "Pre-equalization for pre-rake miso ds-uwb systems," *IEEE International Conference on Communications , ICC '08*, pp. 4861 – 4866, May 2008.

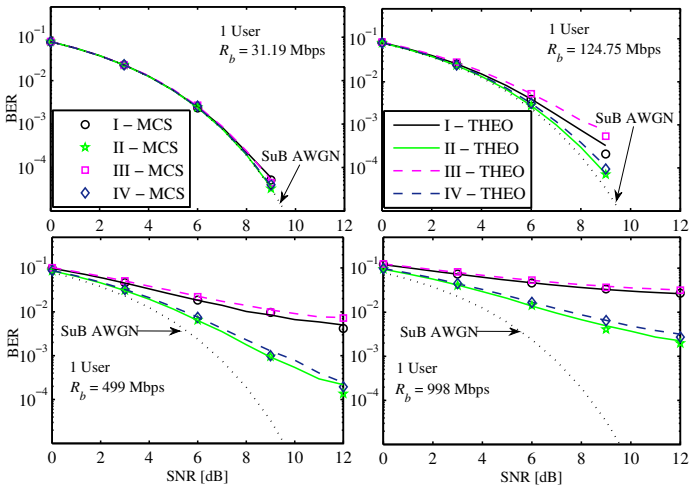

Fig. 4. MCS and THEO BER performances for 1 user, where: I- CM1 and $A_t = 1$; II- CM1 and $A_t = 3$; III- CM3 and $A_t = 1$; IV- CM3 and $A_t = 3$.

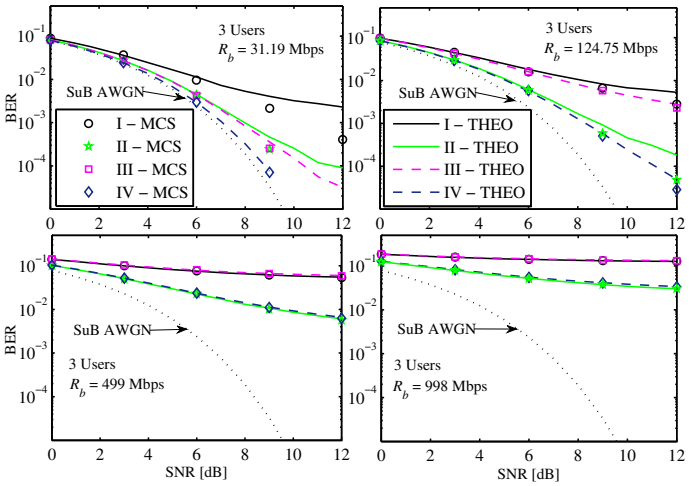

Fig. 5. MCS and THEO BER performances for 3 users, where: I- CM1 and $A_t = 1$; II- CM1 and $A_t = 3$; III- CM3 and $A_t = 1$; IV- CM3 and $A_t = 3$.

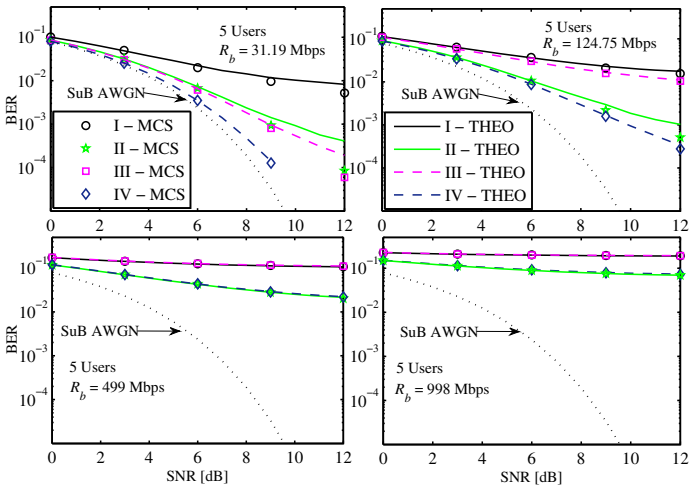

Fig. 6. MCS and THEO BER performances for 5 users, where: I- CM1 and $A_t = 1$; II- CM1 and $A_t = 3$; III- CM3 and $A_t = 1$; IV- CM3 and $A_t = 3$.